

**Table 1**  
Clinical characteristics of patients in this study.

	Pregnant	After delivery	PPH of unknown etiology
No. of subjects	15	18	34
Age (years)	34.0±4.0	37.0±3.0	36.0±4.7
Gravida	1.14±1.10	1.57±0.98	1.08±0.99
Parity	0.79±1.05	1.29±1.11	0.88±0.97
Nulliparous (%)	9 (60.0)	6 (33.3)	23 (67.6)
Multiparous (%)	6 (40.0)	12 (66.6)	11 (32.3)
Gestational age (weeks)	37.8±0.7	38.3±1.5	38.3±2.1
Delivery methods			
Vaginal delivery (%)	0 (0.0)	0 (0.0)	15 (44.1)
Cesarean section (%)	15 (100.0)	18 (100.0)	19 (55.9)
Blood loss at delivery (mL)			
Vaginal delivery	–	–	8723±6757
Cesarean section	–	716±312	8421±6230

Women without previous history of delivery were determined as parity 0.

Immunohistochemistry of C5aR (CD88) showed an increased count of C5a receptor-positive cells within the myometrium in PPH of unknown etiology compared with controls (Fig. 1G–I)

Immunohistochemistry using anti-elastase antibody revealed a significant number of neutrophil infiltration within the uterine myometrium in cases of 'PPH of

unknown etiology' ( $0.04979 \pm 0.01490$  cells/one muscle cell) than in pregnant ( $0.00106 \pm 0.00033$ ) and post-delivery ( $0.00618 \pm 0.00395$ ) groups (Figs. 2D–F and 3C, and Table 2).

Higher number of macrophage infiltration was shown using anti-CD68 antibody ( $0.15826 \pm 0.04183$  cells/one muscle cell) in cases of 'PPH of unknown etiology'

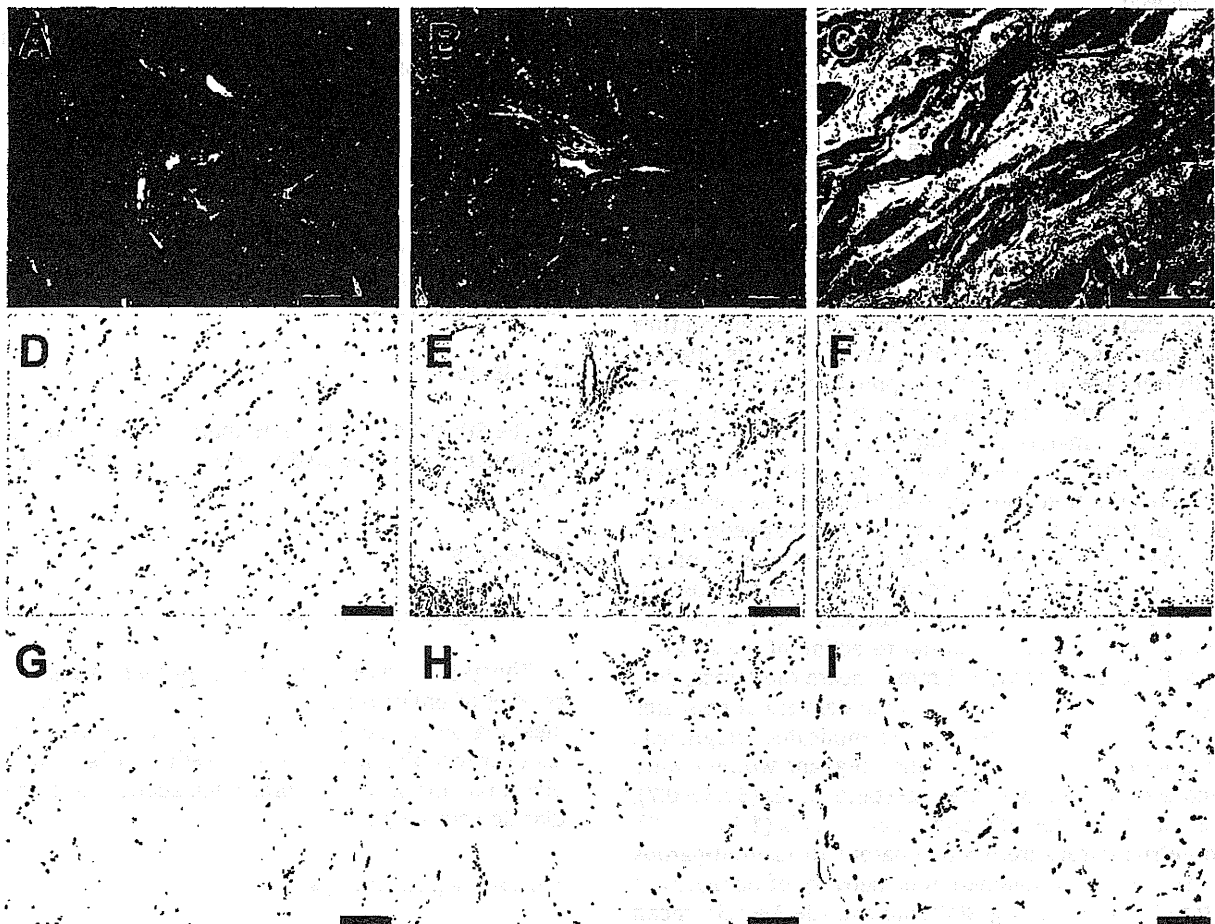


**Fig. 1.** (A) and (D) show representative myometrium during pregnancy without PPH. (B) and (E) from normal myometrium after delivery show slightly edematous interstitium without inflammatory cells. (C) and (F) from a PPH case show inflammatory cell infiltration and interstitial edema. ((A–C): H&E staining, (D–F): Alcian blue staining). Immunohistochemistry of C5aR (CD88) in myometrium from pregnant (G), after delivery (H), and PPH (I) reveal that CD88-positive cells count are significantly high in the PPH group (I). Scale bars indicate 100  $\mu$ m.

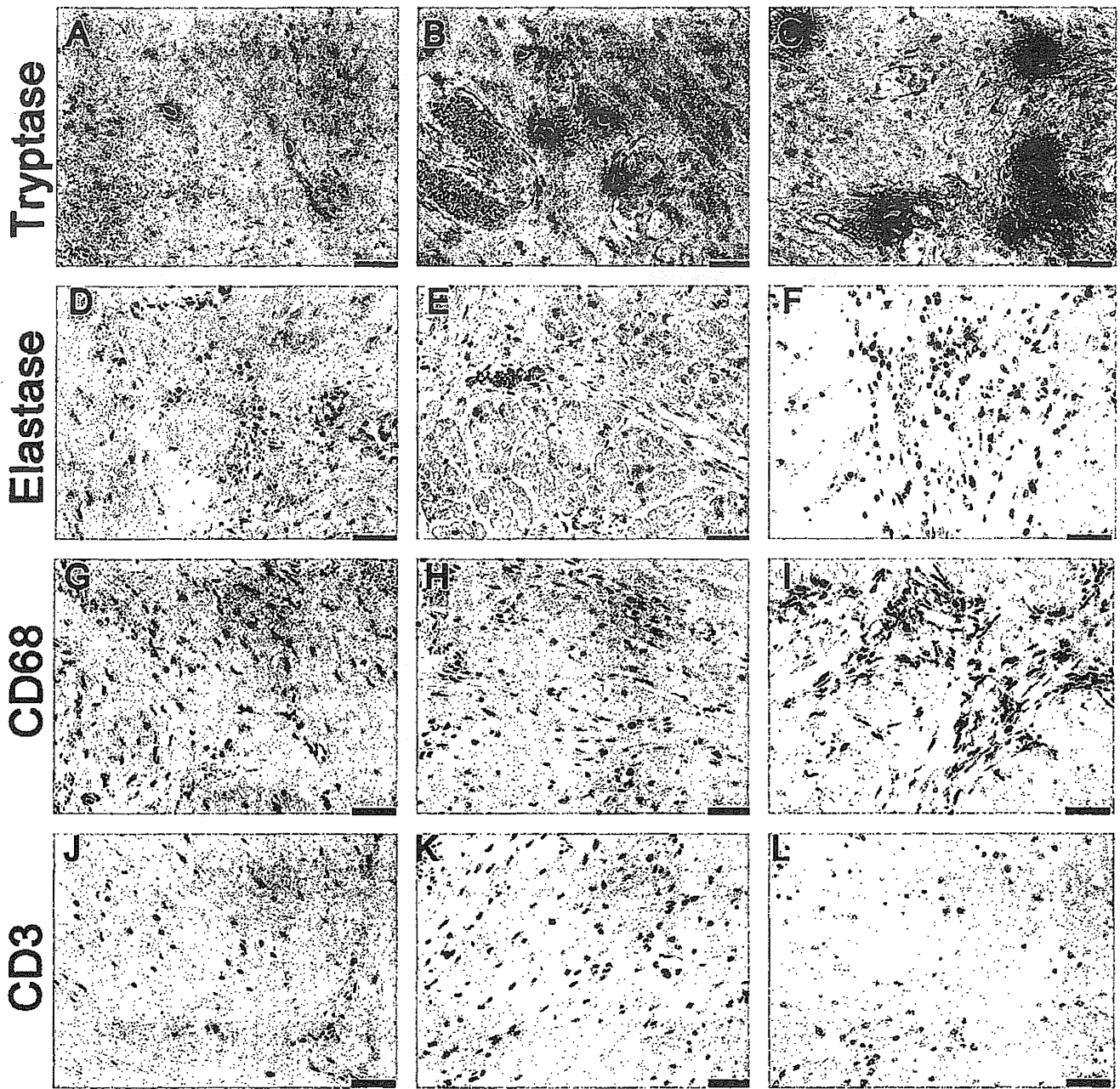


Fig. 2. Immunohistochemistry of mast cell tryptase (A–C), neutrophil elastase (D–F), CD68 (G–I), and CD3 (J–L) in the myometrium during pregnancy (A, D, G, J), after delivery (B, E, H, K), and with PPH (C, F, I, L) show significantly higher number of mast cells (C), neutrophils (F) and macrophages (I) infiltration within the myometrium of PPH compared with the control groups. A golden reaction around mast cells (C) indicates activated mast cell degranulation. Scale bars indicate 50  $\mu$ m.

Table 2  
Summary of exact cell counts in this study.

	Pregnant	After delivery	PPH of unknown etiology
Total mast cells	0.01485 $\pm$ 0.00186	0.02097 $\pm$ 0.00556	0.03395 $\pm$ 0.00242*
Active mast cells	0.00050 $\pm$ 0.00015	0.00444 $\pm$ 0.00129	0.01775 $\pm$ 0.00143*
Neutrophils	0.00106 $\pm$ 0.00033	0.00618 $\pm$ 0.00395	0.04979 $\pm$ 0.01490*
CD68 positive cells (macrophages)	0.00158 $\pm$ 0.00042	0.01234 $\pm$ 0.00483	0.15826 $\pm$ 0.04183*
CD3 positive cells (T cells)	0	0	0

Exact cell counts are presented as the median  $\pm$  SE.

\* Indicates  $p < 0.05$ .

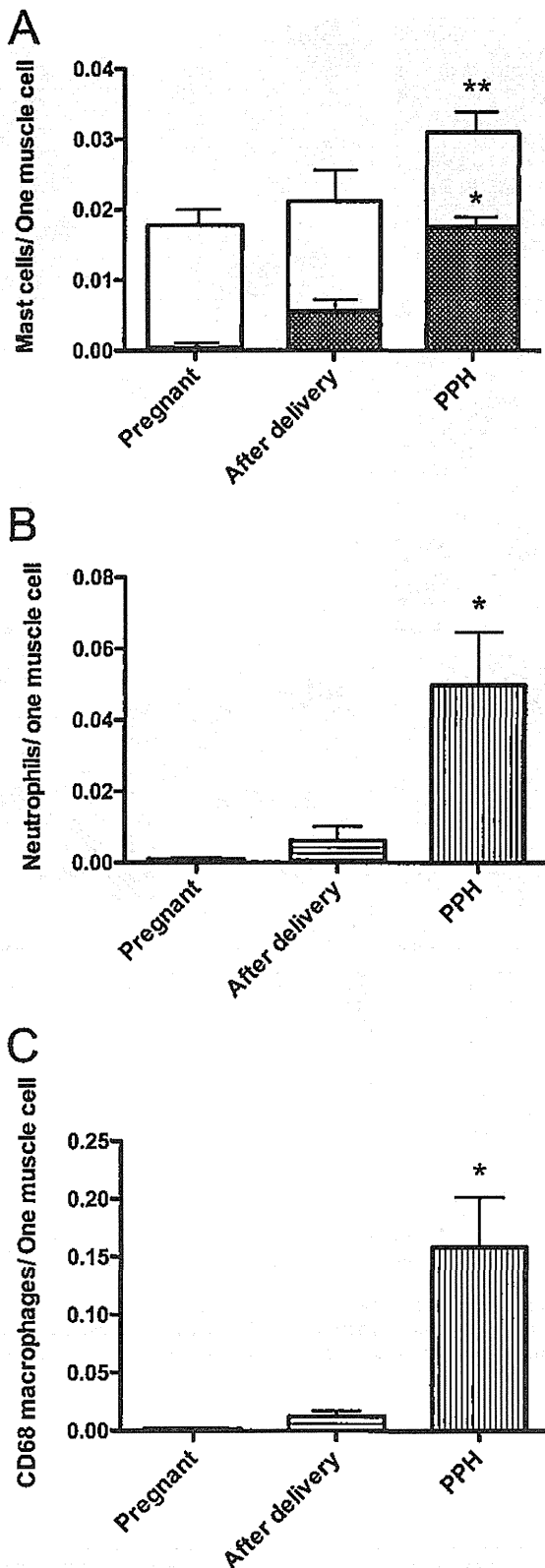


Fig. 3. Columns indicating results for positive cell numbers in the myometrium during pregnancy ( $n=15$ ), after delivery ( $n=18$ ), and with PPH of unknown etiology ( $n=34$ ). The number of tryptase-positive mast cells (A) white and black columns indicated total count of mast cells and activated mast cells respectively), elastase-positive neutrophils (B) and CD68-positive macrophages (C) were significantly higher in the PPH group among the three groups. \*  $P < 0.05$ .

compared with pregnant ( $0.00158 \pm 0.00042$ ) and post-delivery ( $0.01234 \pm 0.00483$ ) groups (Figs. 2G–I and 3D, and Table 2).

Immunohistochemistry using anti-CD3 antibody for T cells revealed equally negative values in all groups (Fig. 2J–L and Table 2).

Total counts of mast cells were significantly high in the 'PPH of unknown etiology' ( $0.03395 \pm 0.00242$  cells/one muscle cell) group than in the pregnant ( $0.01485 \pm 0.00186$ ) and post-delivery ( $0.02097 \pm 0.00556$ ) groups (Figs. 2A–C and 3A, and Table 2). A halo of tryptase positivity around the mast cells (Fig. 2C) indicated activated mast cell degranulation. Activated mast cell counts also increased ( $0.01775 \pm 0.00143$  cells/one muscle cell: 56.5% of total mast cells) in the 'PPH of unknown etiology' group, but not so significant in the pregnant ( $0.00050 \pm 0.00015$ ; 34.0% of total mast cells) and post-delivery ( $0.00444 \pm 0.00129$ ; 2.4% of total mast cells) groups (Fig. 3A and Table 2).

Immunohistochemistry of zinc coproporphyrin derived from meconium was detected in the uterine vessel of the myometrium in 24 women (70%) of PPH of unknown etiology (Supplemental Fig. 1).

#### 4. Discussion

Postpartum hemorrhage is the most common global cause of maternal death (Anderson, 2009; Mercier and Van de Velde, 2008). Seventy percent of PPH corresponds to uterine atony (Karoshi and Keith, 2009). This is the first histological and immunohistochemical study of uterine tissue in cases of 'PPH of unknown etiology' secondary to uterine atony. Our study showed the acute massive infiltration of inflammatory cells such as neutrophils, CD68-positive macrophages, within the myometrium of the uterus in cases of 'PPH of unknown etiology' (Fig. 2F and I). It was suggested that an acute massive inflammatory reaction might lead to deterioration of the contractile function of myometrial cells, resulting in uterine atony with PPH. Inflammatory cells are a major source of chemical mediators with a marked effect on vascular and uterine smooth muscle. The accumulation of fluid along with inflammatory cells within interstitial spaces resulted in stromal edema observed microscopically (Fig. 1C and F). The occurrence of acute myometritis may provide a clue to understanding how myometrial cells stop the synchronized contraction immediately after giving birth to the neonate and placenta by active labor.

It is generally believed that various populations of leukocytes are present not only in the decidua and endometrium, but also in the pregnant myometrium, where these cells are involved in pregnancy maintenance and uterine contraction during labor (Thomson et al., 1999; Ivanisevic et al., 2010; Osman et al., 2003). The present study demonstrated that a significantly higher number of neutrophils, mast cells, and CD68 macrophages are present in the myometrium of PPH compared with the control groups (Fig. 3A–C). These cells were not originally resident but infiltrated from capillaries to interstitial spaces (Fig. 1A–C). Positive findings for elastase, tryptase, and infiltration by activated macrophages

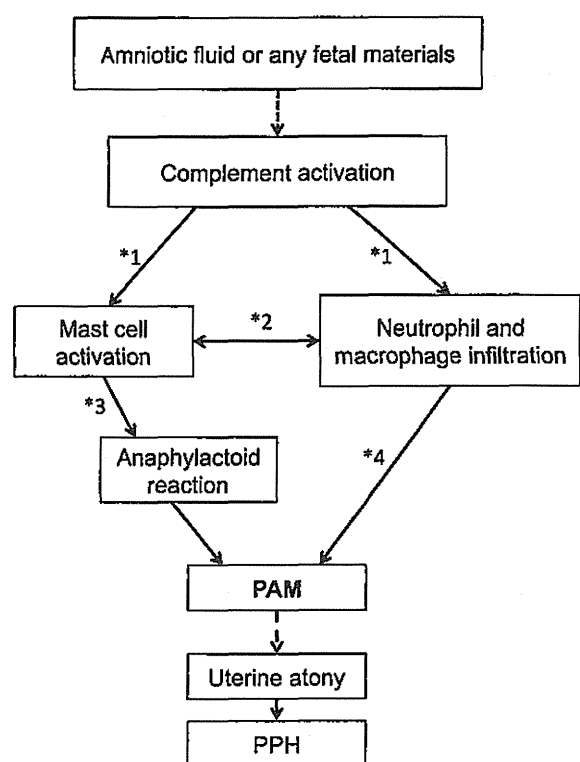


Fig. 4. Scheme indicating the mechanism of pathogenesis in PPH of unknown etiology. \* 1: Anaphylatoxin (C3a, C5a), \* 2: IL-1, IL-8, TNF- $\alpha$ , \* 3: Degranulation of mast cells and \* 4: Matrix metalloproteinase and free radicals were possible components. PAM: Postpartum acute myometritis.

suggested that inflammatory reactions might be accelerated in the myometrium of 'PPH of unknown etiology'. Immunohistochemistry of CD3 and CD8 for T cells revealed equally negative values in all groups. This also suggested an acute onset during or soon after delivery. Cells detected by immunohistochemistry of CD4 (Supplemental Fig. 2) probably infiltrated macrophages, which was also confirmed by CD68 staining (Fig. 2G–I).

Based on the present histological evidence, we termed the condition 'Postpartum Acute Myometritis (PAM)' characterized by 'PPH of unknown etiology.' We propose the following histological criteria for PAM: massive infiltration of inflammatory cells as well as immune cells in the myometrium in the absence of an infective etiology. Complement activation may be the initial step of development of PAM by inflammatory cell infiltration and anaphylactic reaction secondary to mast cell degranulation (Fig. 4). Some researchers have reported evidence of complement involvement in AFE in addition to mast cell involvement in uterine tissue (Benson et al., 2001; Tamura et al., 2014b). In the present study, the increased immunohistochemistry of C5aR (receptor for complement C5) is also supportive of complement activation locally in the myometrium of PPH of unknown etiology (Fig. 1G–I).

We also observed significant activation of mast cells in cases of PPH of unknown etiology and suggested the possibility that myometrial local immune activation might be initiated on encountering foreign substances. Interestingly, immunohistochemistry of meconium-specific ZnCP-I was also observed, especially in relatively large numbers in

'PPH of unknown etiology' (Supplemental Fig. 1), suggesting the possible involvement of the encounter with fetal substances probably originating from amniotic fluid in the local activation of maternal immune reactions in the myometrium. Although there could be several immunological stages during which normal physiological processes are disrupted and contribute to the development of PAM, as described in Fig. 4. We speculated that the presence of amniotic fluid or fetal material in the maternal circulation may stimulate the activation of complement system which might induce myometrial neutrophil and macrophage infiltration, mast cell degranulation and interstitial edema, leading to uterine atony and PPH. Thus, we provide supporting evidence of mast cell degranulation within the uterine myometrium and responsibility for producing an anaphylactic reaction. Of course, further investigations are necessary to clarify the association between myometrial immune activation and fetal components as well as to identify the substance that triggers the reaction.

In conclusion, "PAM", pathologically characterized by evidence of inflammatory cell infiltration and mast cell activation in the myometrium, is a common factor in 'PPH of unknown etiology'. Non-infective etiology such as fetal components is a candidate for a trigger that causes PAM secondary to complements activation. Future studies in this field will pave the way for the early diagnosis of pre-clinical stages related to 'PPH of unknown etiology' and the advancement of treatment.

#### Conflict of interest statement

This manuscript has not been published and is not under consideration for publication elsewhere. All the authors have read the manuscript and have approved this submission and report no conflicts of interest. Financial support for this study was provided by a grant from the Ministry of Education, Culture, Sports, Science, and Technology, Japan (Grant number: 24390379).

#### Acknowledgements

The authors thank Mrs. Naoko Hakamada, Mrs. Yumiko Yamamoto, and Mrs. Naoko Kondo, for secretarial assistance. This work was supported in part by Grants-in-aid for Scientific Research from the Ministry of Education, Culture, Sports, Science, and Technology, Japan (Grant number: 24390379).

#### Appendix A. Supplementary data

Supplementary data associated with this article can be found, in the online version, at <http://dx.doi.org/10.1016/j.jri.2015.04.004>.

#### References

- Anderson, F.W., 2009. Maternal mortality: an enduring epidemic. *Clin. Obstet. Gynecol.* 52, 214–223.
- Benson, M.D., 2007. A hypothesis regarding complement activation and amniotic fluid embolism. *Med. Hypotheses* 68, 1019–1025.
- Benson, M.D., 2012. Current concepts of immunology and diagnosis in amniotic fluid embolism. *Clin. Dev. Immunol.* 2012, 946576.

- Benson, M.D., Kobayashi, H., Silver, R.K., Oi, H., Greenberger, P.A., Terao, T., 2001. Immunologic studies in presumed amniotic fluid embolism. *Obstet. Gynecol.* 97, 510–514.
- Chapter 34, Obstetrical hemorrhage. In: Cunningham, F.G., Leveno, K.J., Bloom, S.L., Hauth, J.C., Rouse, D.J., Spong, C.Y. (Eds.), *Williams Obstetrics*, 23rd ed. McGraw-Hill, New York, 2010, pp. 757–803.
- Fineschi, V., Riezzo, I., Cantatore, S., Pomara, C., Turillazzi, E., Neri, M., 2009. Complement C3a expression and tryptase degranulation as promising histopathological tests for diagnosing fatal amniotic fluid embolism. *Virchows Arch.* 454, 283–290.
- Furuta, N., Yaguchi, C., Itoh, H., Morishima, Y., Tamura, N., Kato, M., Uchida, T., Suzuki, K., Sugihara, K., Kawabata, Y., Suzuki, N., Sasaki, T., Horiuchi, K., Kanayama, N., 2012. Immunohistochemical detection of meconium in the fetal membrane, placenta and umbilical cord. *Placenta* 33, 24–30.
- Ivanisevic, M., Segerer, S., Rieger, L., Kapp, M., Dietl, J., Kammerer, U., Frambach, T., 2010. Antigen-presenting cells in pregnant and non-pregnant human myometrium. *Am. J. Reprod. Immunol.* 64, 188–196.
- Kanayama, N., Tamura, N., 2014. Amniotic fluid embolism: pathophysiology and new strategies for management. *J. Obstet. Gynaecol. Res.* 40, 1507–1517.
- Kanayama, N., Inori, J., Ishibashi-Ueda, H., Takeuchi, M., Nakayama, M., Kimura, S., Matsuda, Y., Yoshimatsu, J., Ikeda, T., 2011. Maternal death analysis from the Japanese autopsy registry for recent 16 years: significance of amniotic fluid embolism. *J. Obstet. Gynaecol. Res.* 37, 58–63.
- Karoshi, M., Keith, L., 2009. Challenges in managing postpartum hemorrhage in resource-poor countries. *Clin. Obstet. Gynecol.* 52, 285–298.
- Mercier, F.J., Van de Velde, M., 2008. Major obstetric hemorrhage. *Anesthesiol. Clin.* 26, 53–66, vi.
- Mousa, H.A., Blum, J., Abou, E.L., Senoun, G., Shakur, H., Alfirevic, Z., 2014. Treatment for primary postpartum haemorrhage. *Cochrane Database Syst. Rev.* 2, Cd003249.
- Osman, I., Young, A., Ledingham, M.A., Thomson, A.J., Jordan, F., Greer, I.A., Norman, J.E., 2003. Leukocyte density and pro-inflammatory cytokine expression in human fetal membranes, decidua, cervix and myometrium before and during labour at term. *Mol. Hum. Reprod.* 9, 41–45.
- Oyelese, Y., Ananth, C.V., 2010. Postpartum hemorrhage: epidemiology, risk factors, and causes. *Clin. Obstet. Gynecol.* 53, 147–156.
- Oyelese, Y., Scorza, W.E., Mastroli, R., Smulian, J.C., 2007. Postpartum hemorrhage. *Obstet. Gynecol. Clin. North Am.* 34, 421–441, x.
- Rouse, D.J., Macpherson, C., Landon, M., Varner, M.W., Leveno, K.J., Moawad, A.H., Spong, C.Y., Caritis, S.N., Meis, P.J., Wapner, R.J., Sorokin, Y., Miodovnik, M., Carpenter, M., Peaceman, A.M., O'Sullivan, M.J., Sibai, B.M., Langer, O., Thorp, J.M., Ramin, S.M., Mercer, B.M., 2006. Blood transfusion and cesarean delivery. *Obstet. Gynecol.* 108, 891–897.
- Tamura, N., Kimura, S., Farhana, M., Uchida, T., Suzuki, K., Sugihara, K., Itoh, H., Ikeda, T., Kanayama, N., 2014a. CI esterase inhibitor activity in amniotic fluid embolism. *Crit. Care Med.* 42, 1392–1396.
- Tamura, N., Nagai, H., Maeda, H., Kuroda, R.H., Nakajima, M., Igarashi, A., Kanayama, N., Yoshida, K.I., 2014b. Amniotic fluid embolism induces uterine anaphylaxis and atony following cervical laceration. *Gynecol. Obstet. Invest.* 78, 65–68.
- Thomson, A.J., Telfer, J.F., Young, A., Campbell, S., Stewart, C.J., Cameron, I.T., Greer, I.A., Norman, J.E., 1999. Leukocytes infiltrate the myometrium during human parturition: further evidence that labour is an inflammatory process. *Hum. Reprod.* 14, 229–236.



Original contribution

# Morphologic characteristics of the placental basal plate in in vitro fertilization pregnancies: a possible association with the amount of bleeding in delivery<sup>☆</sup>



Yuki Nakamura MD<sup>a,1</sup>, Chizuko Yaguchi MD<sup>a,1</sup>, Hiroaki Itoh MD, DMedSci<sup>a,\*</sup>,  
Ryoko Sakamoto BS<sup>a</sup>, Takako Kimura CT<sup>a</sup>, Naomi Furuta MD<sup>a</sup>,  
Toshiyuki Uchida MD, PhD<sup>a</sup>, Naoaki Tamura MD, PhD<sup>a</sup>, Kazunao Suzuki MD, PhD<sup>a</sup>,  
Kazuhiro Sumimoto PhD<sup>b</sup>, Yumiko Matsuda CT<sup>c</sup>, Toshiki Matsuura MD, PhD<sup>c</sup>,  
Mitsuru Nishimura MD, PhD<sup>d</sup>, Naohiro Kanayama MD, PhD<sup>a</sup>

<sup>a</sup>Department of Obstetrics and Gynecology, Hamamatsu University School of Medicine, Hamamatsu 431-3192, Japan

<sup>b</sup>Tsuruga Nursing University, Tsuruga 914-0814, Japan

<sup>c</sup>ACT Tower Clinic, Hamamatsu 430-7707, Japan

<sup>d</sup>Nishimura Women's Clinic, Hamamatsu 433-8122, Japan

Received 5 December 2014; revised 6 April 2015; accepted 8 April 2015

## Keywords:

Placenta;  
Pregnancy;  
Delivery;  
Postpartum hemorrhage  
(PPH);  
Assisted reproductive  
technology (ART)

**Summary** The aim of the present study was to investigate the relationship between assisted reproductive technology procedures, the morphology of the basal plate of placentas, and amount of bleeding in deliveries. Fifty-five whole placentas (fresh-embryo transfer in the in vitro fertilization cycle [n = 6], frozen-thawed embryo transfer in the natural cycle [n = 13] or in the hormonal cycle [n = 10], and age-matched spontaneously conceived pregnancies [n = 26]) were retrospectively enrolled and histologically analyzed. The whole placentas were stored in our pathological division among 512 singleton pregnancies with vaginal deliveries (34–41 weeks of gestation) at Hamamatsu University Hospital. The morphology of the placental basal plate was examined using Azan staining. A total of 20 digital images (each 0.53 mm<sup>2</sup>) of microscopic fields were analyzed per placenta to measure the mean values of the vertical maximum thickness of Rohr and Nitabuch fibrinoid layers and % loss of decidua. The thickness of Rohr fibrinoid layer and % loss of decidua were significantly higher in the frozen-thawed embryo transfer in the hormonal cycle group than in the frozen-thawed embryo transfer in the natural cycle and spontaneously conceived pregnancy groups (each *P* < .01). The z scores for both the thickness of Rohr fibrinoid layer and % loss of decidua positively correlated with those for the amount of bleeding in deliveries (*P* < .05 each). Assisted reproductive technology procedures changed the morphology of the placental basal plate, suggesting a possible association with an increase in the amount of bleeding in deliveries.  
© 2015 Elsevier Inc. All rights reserved.

<sup>☆</sup> Funding/Support: This study was supported, in part, by Grants-in-Aid for Scientific Research from the Ministry of Education, Science, Culture and Sports, Japan (No. 25670490 and No. 24390273).

\* Corresponding author at: Department of Obstetrics and Gynecology, Hamamatsu University School of Medicine, 1-20-1 Handayama, Higashi-ku, Hamamatsu 341-3192, Japan.

E-mail address: hitou-endo@umin.ac.jp (H. Itoh).

<sup>1</sup> Contributed equally to this study.

## 1. Introduction

Assisted reproductive technology (ART) has been widely used for more than a decade to treat infertility. It currently remains unclear whether ART procedures and/or infertility-

associated factors contribute to adverse outcomes [1–11]. The adverse effects associated with ART in singleton pregnancies have mainly been examined in relation to preterm deliveries, fetal growth restriction, and perinatal mortality [2,3], but few have investigated the relationship between the amount of bleeding in deliveries and ART procedures. Schieve et al [12] reported that ART pregnancies were associated with uterine bleeding; however, the diagnostic criteria of “uterine bleeding” were not described. Hayashi et al [13] reported a significant increase in postpartum hemorrhage in ART pregnancies. Although these limited findings suggested a possible association between ART procedures and the amount of bleeding in deliveries, a consensus has not yet been established.

The blastocyst differentiates into the inner cellular mass or trophoblast (TE), and the inner cellular mass and trophoblast eventually form the fetal and placental compartments, respectively [14]. Therefore, it is plausible that not only the fetus but also the placenta may be predisposed to the effects of ART procedures during the early stage of gestation. However, only a few differences have been reported in the placental morphologies of ART pregnancies, such as marginal and velamentous cord insertion and an abnormal placental shape (assessed by the closest placental margin) [15–20].

A hematoma commonly forms between the separating placenta and placental bed as placental separation proceeds, and this hematoma markedly contributes to the amount of total bleeding in delivery; however, this is negligible in some cases [21]. Therefore, morphologic changes in the basal plate of the placenta of ART pregnancies, if present, may be associated with the amount of bleeding. We herein focused on the potential effects of ART procedures on the morphology of the placental basal plate in association with the amount of bleeding in deliveries.

We hypothesized that ART procedures may change the morphology of the basal plates of placentas and be causatively associated with an increase in the amount of bleeding in deliveries. To examine these hypotheses, we retrospectively investigated morphologic changes in the basal plates of placentas (ie, the thickness of Rohr and Nitabuch fibrinoid layers [22–25] and % loss of decidua) as well as the amount of bleeding in deliveries, and then assessed their relationships with ART procedures in pregnancies achieved by fresh-embryo transfer in the in vitro fertilization (IVF) cycle, frozen-thawed embryo transfer in the natural cycle, and frozen-thawed embryo

transfer in the hormonal cycle as well as age-matched spontaneously conceived pregnancies.

## 2. Materials and methods

### 2.1. Subjects

Fifty-five whole placentas (fresh-embryo transfer in the IVF cycle [ $n = 6$ ], frozen-thawed embryo transfer in the natural cycle [ $n = 13$ ] or in the hormonal cycle [ $n = 10$ ], and age-matched spontaneously conceived pregnancies [ $n = 26$ ]) were retrospectively enrolled and histologically analyzed. Three placentas (frozen-thawed embryo transfer in the hormonal cycle) were not enrolled because they were complicated with placenta accreta. The clinical backgrounds of these placentas were obtained from clinical records and summarized in the Table. These whole placentas were stored in our pathological division among 512 singleton pregnancies with vaginal deliveries at Hamamatsu University Hospital between February 2010 and February 2013 (34–41 weeks of gestation). The clinical backgrounds of these 512 singleton pregnancies were obtained from clinical records and summarized in Supplementary Table 2. Subjects were not enrolled if clinical records showed maternal complications including congenital uterine malformations, myoma uteri, adenomyosis, a history of myomectomy when the uterine incision had reached the endometrium, preeclampsia, gestational hypertension, gestational diabetes mellitus, and thrombocytopenia. Cases of vaginal birth after cesarean section were not enrolled.

The amount of bleeding in vaginal deliveries was counted between delivery of the neonate and 2 hours subsequent to delivery of the placenta.

### 2.2. ART procedures

IVF-embryo transfer was performed at 3 institutions: Hamamatsu University Hospital (Hamamatsu Japan), ACT Tower Clinic (Hamamatsu, Japan), and Nishimura Women's Clinic (Hamamatsu, Japan). Fresh embryos were transferred during the IVF cycle, whereas frozen-thawed embryos were transferred during either the natural or hormonal cycle. The oral administration of chlormadinone acetate (6 and 12 mg/d, before and after embryo transfer, respectively) and the

**Table** Embryo transfer cycle, backgrounds, and amount of bleeding in vaginal deliveries, from which the placentas were histologically analyzed

Embryo transfer cycle	Embryo	n	Maternal age (y)	Weeks of gestation	Birth weight (g)	Bleeding in vaginal deliveries (mL)
IVF cycle	Fresh	6	34.8 ± 3.3 (29-39)	38.8 ± 0.8 (38-40)	2817.7 ± 562.9 (2284-3650)	597.2 ± 592.1 (100-1460)
Natural cycle	Frozen thawed	13	34.5 ± 3.3 (28-39)	39.4 ± 1.4 (37-41)	3003.5 ± 162.9 (2578-3208)	425.2 ± 314.8 (22-998)
Hormonal cycle	Frozen thawed	10	34.3 ± 3.0 (31-39)	38.3 ± 2.0 (34-41)	2826.2 ± 526.7 (2006-3490)	1098.2 ± 700.4* (175-2430)
Spontaneously conceived pregnancy		26	34.2 ± 4.2 (28-45)	39.0 ± 1.4 (35-41)	2941.5 ± 435.2 (1974-3796)	859.7 ± 868.2 (70-4050)

NOTE. Values are the mean ± SD.

\*  $P < .05$  vs the spontaneously conceived pregnancy group.

percutaneous administration of estradiol (1.42 mg/2 days) were used in hormonal cycle cases. No hormonal treatment was administered after oocyte pick-up in fresh-embryo transfer during the IVF cycle or in frozen-thawed embryo transfer during the natural cycle.

### 2.3. Preparation for histologic examination of the placenta

Of the 512 enrolled singleton pregnancies by vaginal delivery, 55 whole placentas were stored in our pathological division after being vacuum sealed in plastic packages with 10% formaldehyde. The systemic random sampling of vacuum-sealed whole placentas was conducted according to the method of Mayhew [22] by 2 medical students (Chika Masuda and Fukue Kondo) who were blind to the study population. In brief, 4 paraffin blocks were systematically obtained from a placenta, as described by Mayhew [22]. Each block was made vertically from the maternal side to the fetal side and cut into 200 to 400 serial sections (3  $\mu\text{m}$ ), from which 1 section was randomly selected [22]. Four sections per placenta were used in each cohort.

### 2.4. Standard assessment of placental histology

A gross morphologic survey was performed and pathological abnormalities were examined by 2 researchers (N. Furuta and Yaguchi C.) using hematoxylin and eosin (HE) staining [20,23].

### 2.5. Immunohistochemistry of the placental basal plate

An antifibrinogen mouse monoclonal antibody (ab58207; Abcam Japan, Tokyo, Japan), antifibronectin mouse monoclonal antibody (ab32419; Abcam Japan), antivimentin mouse monoclonal antibody (ab24988; Abcam Japan), or anticytokeratin mouse monoclonal antibody (ab24988; Abcam Japan) was applied to the sections, and detection was performed with a polymer detection kit (ChemMate EnVision; Dako Japan, Tokyo, Japan), as described previously [24]. This was followed by a reaction with 3,3'-diaminobenzidine and counterstaining with hematoxylin.

### 2.6. Histologic assessment of the placental basal plate

The morphology of the placental basal plate was closely examined using Azan staining of 4 sections per whole placenta, which were obtained by systemic random sampling, as described above. Five microscopic fields (each 0.53  $\text{mm}^2$ ) including a portion of the basal plate were arbitrarily selected in each of the 4 sections, and digital images were recorded. A total of 20 digital images of the microscopic fields were then analyzed per placenta.

Immunostaining for fibronectin as well as fibrinogen was used to confirm Rohr and Nitabuch fibrinoid layers (Fig. 1) [25]. After comparisons with immunostaining, we applied Azan staining to assess the thicknesses of Rohr and Nitabuch fibrinoid layers. The vertical maximum thicknesses of Rohr (Fig. 2A and B) and Nitabuch (Fig. 3A and B) fibrinoid layers were measured in each of the 20 digital images of the microscopic fields of a placenta. Mean values were regarded as the thicknesses of Rohr and Nitabuch fibrinoid layers in a placenta, respectively.

A decidua-free margin was also confirmed by immunostaining for vimentin (Fig. 4). After comparisons with immunostaining, we applied Azan staining to assess a decidua-free margin. The total length of the decidua-free placental margin (Fig. 5B) in 20 microscopic fields of a placenta was divided by the total length of the placental margin in identical microscopic fields (Fig. 5A and B) and was regarded as the % loss of decidua in a placenta.

### 2.7. Statistical analysis

Data are expressed as means  $\pm$  SDs. The *z* scores were calculated by using the formula  $([\text{datum} - \text{mean of the population}]/[\text{SD of the population}])$ . Significant differences among more than 3 mean values were assessed using the Steel-Dwass test. Pearson correlation coefficient was calculated between parameters. Fisher exact test was carried out to determine whether there was a significant difference in the data collected. A *P* value less than .05 was regarded as significant.

### 2.8. Approval

The Ethics Committee of the Hamamatsu University School of Medicine approved all the procedures used in this study (No. 24-265).

## 3. Results

### 3.1. Thickness of Rohr fibrinoid layer in the placental basal plate

The mean thickness of Rohr fibrinoid layer (Fig. 2A and B) was significantly higher in the frozen-thawed embryo transfer in hormonal cycle group than in the frozen-thawed embryo transfer in the natural cycle and spontaneously conceived pregnancy groups (Fig. 2C). The *z* scores for the thickness of Rohr fibrinoid layer positively correlated with those for the amount of bleeding in deliveries (Fig. 2D).

### 3.2. Thickness of Nitabuch fibrinoid layer in the placental basal plate

No significant difference was observed in the mean thickness of Nitabuch fibrinoid layer (Fig. 3A and B) among the frozen-thawed embryo transfer in hormonal cycle, fresh-embryo



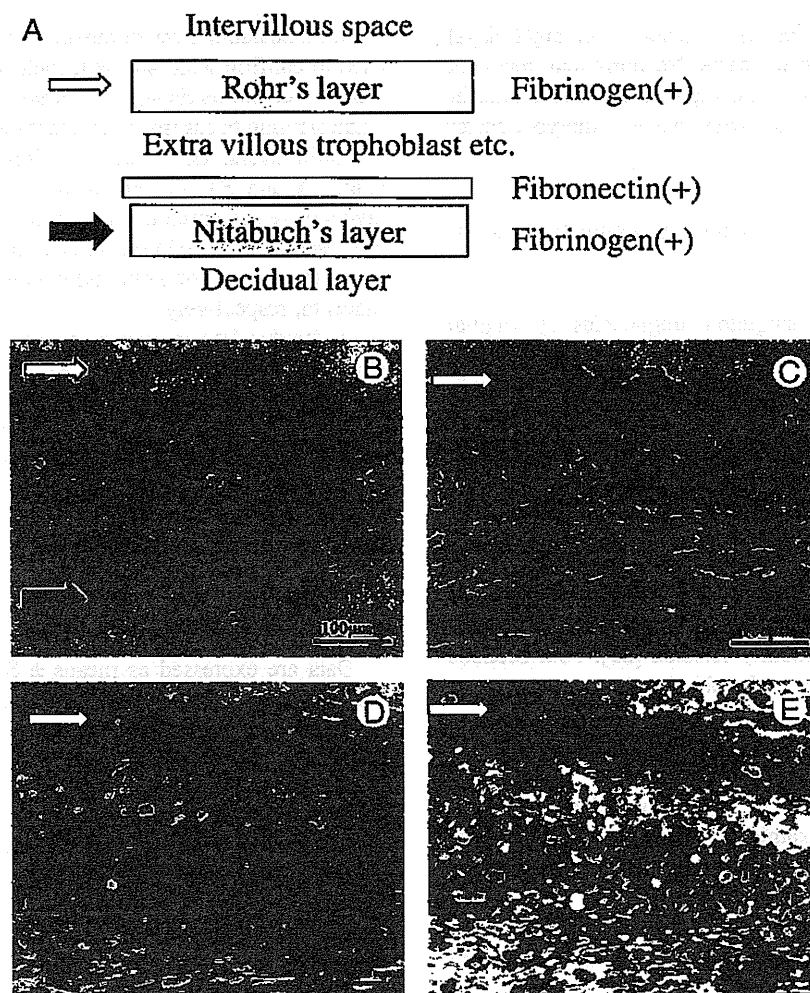


Fig. 1 A, Schematic illustration of Rohr and Nitabuch fibrinoid layers. Immunohistochemistry of fibronectin (B) and fibrinogen (C) and HE (D) and Azan (E) staining of serial sections in the placental basal plate. White and black arrows indicate Rohr and Nitabuch fibrinoid layers, respectively.

transfer in the IVF cycle, frozen-thawed embryo transfer in the natural cycle, and spontaneously conceived pregnancy groups (Fig. 3C). The z scores for the thickness of Nitabuch fibrinoid layer did not correlate with those for the amount of bleeding in deliveries (Fig. 3D).

### 3.3. Percent loss of decidua in the placental basal plate

The mean % loss of decidua (Fig. 5A and B) was significantly higher in the frozen-thawed embryo transfer in the hormonal cycle group than in the fresh-embryo transfer in the IVF cycle, frozen-thawed embryo transfer in the natural cycle, and spontaneously conceived pregnancy groups (Fig. 5C). The z scores for the % loss of decidua positively correlated with those for the amount of bleeding in deliveries (Fig. 5D).

### 3.4. Other observations in the placental basal plate

No apparent differences were observed in the morphology of the decidual vessels among 4 study groups (representative HE staining is shown in Supplementary Fig. 1). There were no statistical significant differences in the average vessel areas in decidua (Supplementary Fig. 2).

Immunostaining for cytokeratin was carried out to assess extravillous trophoblasts. No significant morphologic differences were noted among the 4 study groups (representative immunostaining is shown in Supplementary Fig. 3). There were no statistical significant differences in the average thickness of extravillous trophoblast layer (Supplementary Fig. 4).

### 3.5. Standard assessment of placental histology

Supplementary Table 1A and B show the standard assessment of placental histology and placental weight,

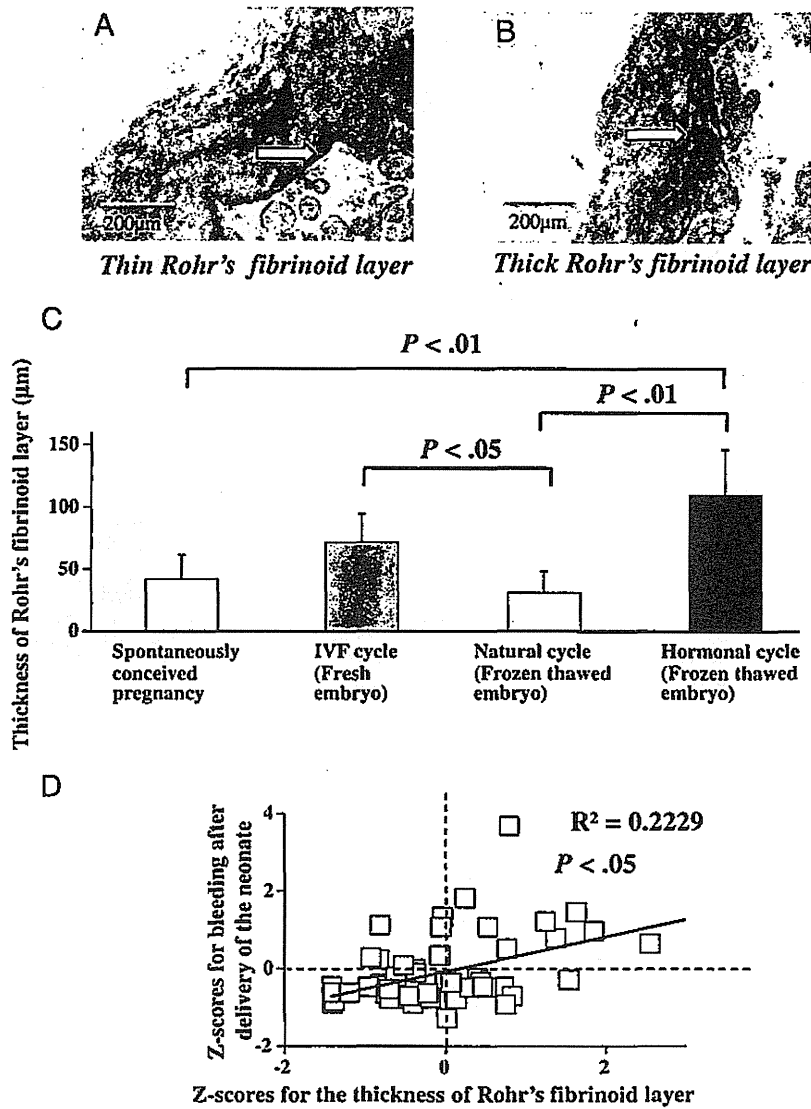


Fig. 2 Azan staining of the basal plate of the placenta showing a thin (white arrow; A) or thick (white arrow; B) Rohr fibrinoid layer, and a comparison of the mean thickness of Rohr fibrinoid layer (C). D, Relationships between z scores for the amount of bleeding in vaginal deliveries and thickness of Rohr fibrinoid layer in the placental basal plate (white squares). Error bars represent SD of the mean thickness of Rohr fibrinoid layer (in micrometers; C).

respectively. No significant difference was observed among the 4 study groups.

### 3.6. Amount of bleeding in deliveries

Of the 55 enrolled placentas, the amount of bleeding was significantly larger in the frozen-thawed embryo transfer in the hormonal cycle group than in the spontaneously conceived pregnancy group, from which placentas were stored and histologically analyzed in the present study (Table). Of the 512 enrolled singleton pregnancies by vaginal delivery, the amount of bleeding in vaginal deliveries was significantly larger in the frozen-thawed embryo transfer in the hormonal cycle group

than in the fresh-embryo transfer in the IVF cycle, frozen-thawed embryo transfer in the natural cycle, and spontaneously conceived pregnancy groups (Supplementary Table 2).

## 4. Discussion

In the present study, we conducted a stereologic analysis of the morphologic characteristics in the placental basal plate with or without ART procedures by combining systemic random sampling according to the method of Mayhew [22] and arbitrary selection of 20 digital images of the microscopic fields as described in Materials and Methods.

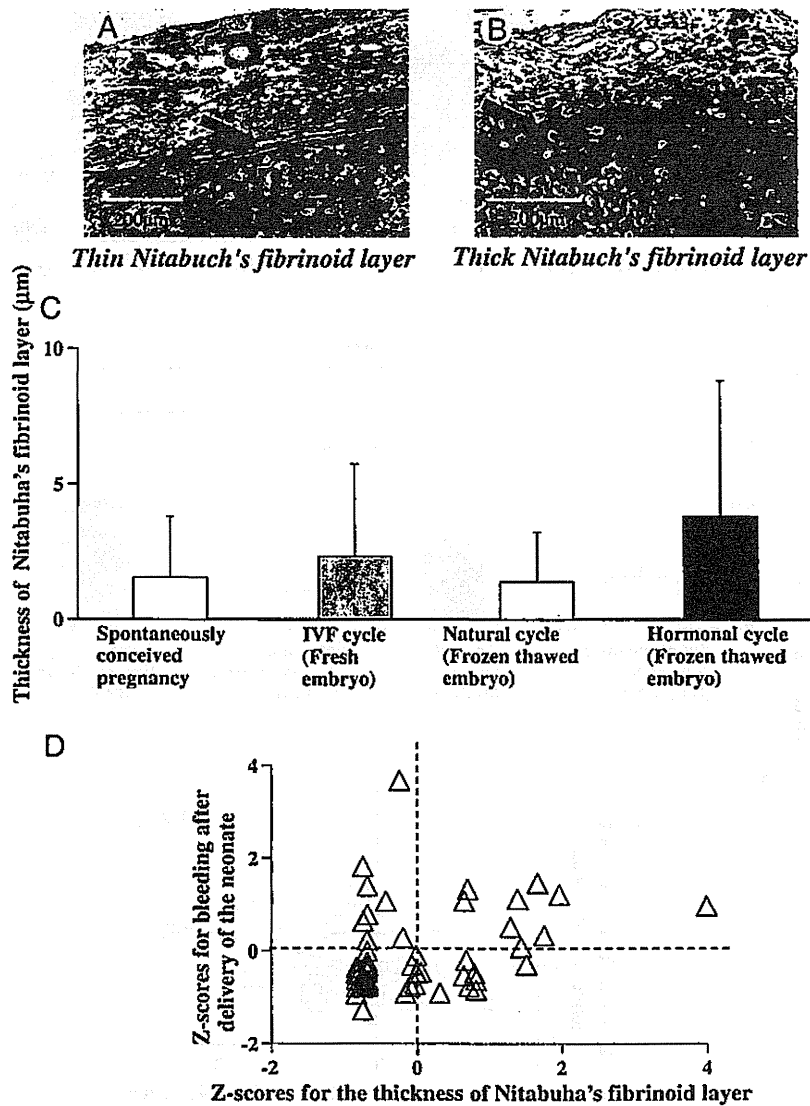


Fig. 3 Azan staining of the basal plate of the placenta showing a thin (black arrow; A) or thick (black arrow; B) Nitabuch fibrinoid layer, and a comparison of the mean thickness of Nitabuch fibrinoid layer (C). D, Relationships between z scores for the amount of bleeding in vaginal deliveries and thickness of Nitabuch fibrinoid layer in the placental basal plate (white triangles). Error bars represent SD of the mean thickness of Nitabuch fibrinoid layer (in micrometers; C).

Rohr fibrinoid layer is located between the villous structure and extravillous trophoblast layer [25–27] (Figs. 1 and 2A and B). The present study showed that the mean thickness of Rohr fibrinoid layer was significantly higher in the frozen-thawed embryo transfer in the hormonal cycle group than that in the frozen-thawed embryo transfer in the natural cycle and spontaneously conceived pregnancy groups (Fig. 2C). Moreover, z scores for the mean thickness of Rohr fibrinoid layer positively correlated with those for the total amount of bleeding in deliveries (Fig. 2D). To the best of our knowledge, this is the first study to report changes in the thickness of Rohr fibrinoid layer in any situation. Because Rohr fibrinoid layer is not located in the placental

separation zone of the decidual layer [25–27], we speculated that unidentified factors associated with determining the thickness of Rohr fibrinoid layer during frozen-thawed embryo transfer in the hormonal cycle may have indirectly affected bleeding during placental separation. Fibrinoid layers in the placental basal plate may play a role in the barrier that protects fetal antigens from being identified by maternal cells [25]. Sutcliffe et al [28] reported the presence of ample fibrinoid layers in human and rodent placentas with invasive implantation relative to other mammals by noninvasive implantation with largely intact maternal and fetal epithelial surfaces facing each other. Based on these findings, it was suggested that changes in the thickness of

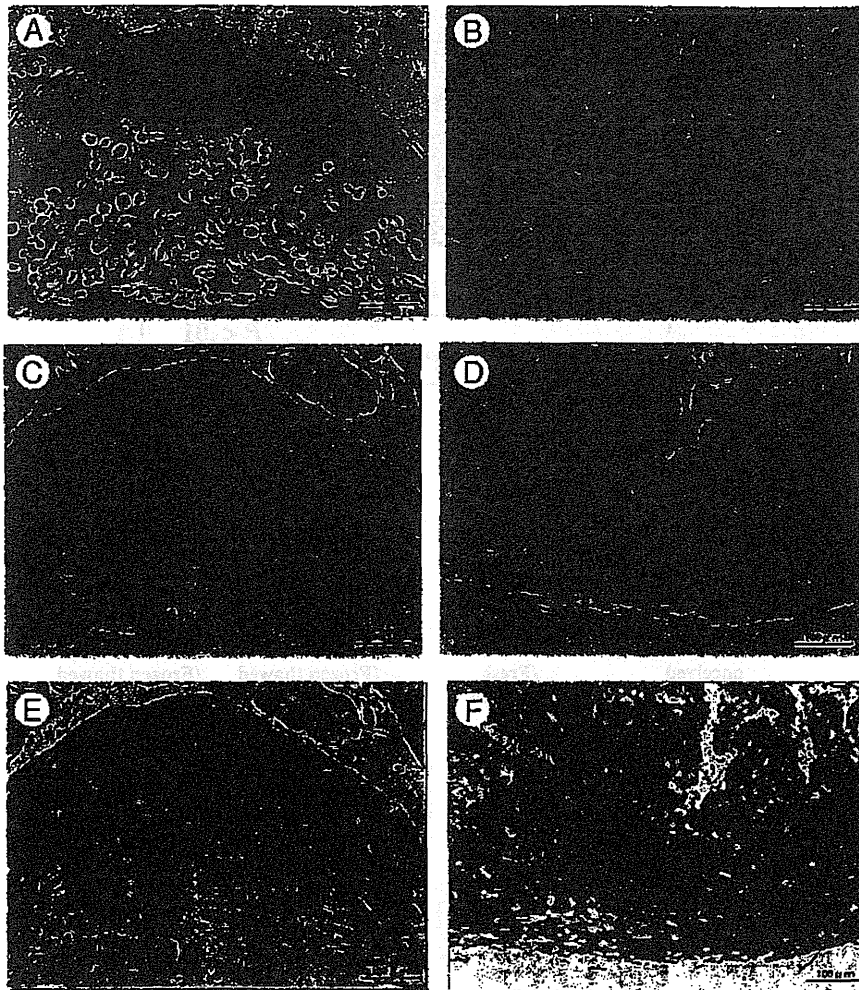


Fig. 4 Immunohistochemistry of vimentin (A and B), HE (C and D), and Azan (E and F) staining in the presence (A, C, and E) or absence (B, D, and F) of a portion of the decidual layer.

Rohr fibrinoid layer might be associated with a fetomaternal immunoreaction or the situation of implantation. More detailed studies are necessary to prove this speculation.

Nitabuch fibrinoid layer is located between the decidual and extravillous trophoblast layers [25,29] (Figs. 1 and 3A and B). No significant difference was observed in the mean thickness of Nitabuch fibrinoid layer (Fig. 3C) among the study groups. Furthermore, no positive correlation was detected between  $z$  scores for the mean thickness of Nitabuch fibrinoid layer and those for the total amount of bleeding in deliveries (Fig. 3D).

Placental separation in the middle of the decidual layer commonly occurs after the delivery of neonates and is also referred to as the *separation zone* [25]. Therefore, 2 different situations are commonly observed in the margin of the placental basal plate, that is, Nitabuch fibrinoid layer with

(Figs. 4 and 5A) or without a neighboring decidual layer (Figs. 4 and 5B). We assessed the % loss of decidua in placentas and found that it was significantly higher in the frozen-thawed embryo transfer in the hormonal cycle group than in the 3 other groups (Fig. 5C). A hematoma commonly forms at the "separation zone" in the decidual layer [25] and markedly contributes to the amount of total bleeding in deliveries [21]. The present study showed that  $z$  scores for the % loss of decidua positively correlated with those for the total amount of bleeding in deliveries (Fig. 5D). Because the decidual layer is a loose spongy structure in which cells are loosely attached to each other by fibrillar networks [30], we speculated that artificial endocrinologic circumstances in early pregnancy, especially frozen-thawed embryo transfer in the hormonal cycle group, may cause changes in the structure and/or function of the extracellular matrix in the decidual layer, as

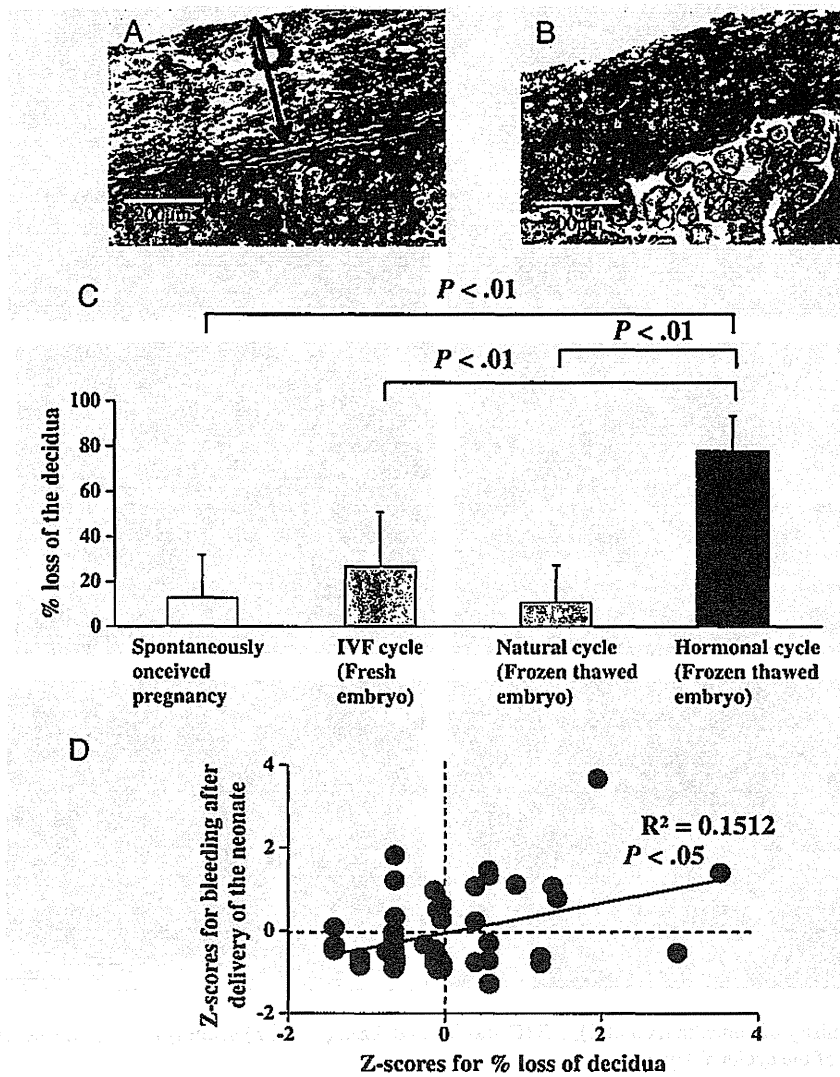


Fig. 5 Azan staining of the basal plate of the placenta showing the presence (black arrow; A) or absence (B) of the decidua layer, and a comparison of the % loss of decidua (C). D, Relationships between z scores for the amount of bleeding in vaginal deliveries and % loss of decidua in the placental basal plate (black circles). Error bars represent SD of the % loss of decidua (C).

represented by the % loss of decidua, and causatively be associated with increased bleeding in deliveries. To the best of our knowledge, this is the first study to report changes in the pattern of attachment of the decidua in any situation.

The present study showed that frozen-thawed embryo transfer in the hormonal cycle increased the amount of bleeding in vaginal deliveries (Table and Supplementary Table 2). Although the numbers in our cohort were small, our results are consistent with previous findings [12,13]. These results together with morphologic observations lead us to speculate that frozen-thawed embryo transfer in the hormonal cycle may increase the amount of bleeding in deliveries at least partly via morphologic changes to the placental basal plate, such as an increase in the thickness of Rohr fibrinoid layer and/or an increase in the % loss of decidua.

Limitations in the present study include the small number of ART subjects as well as placentas analyzed and the retrospective analysis of placentas stored without a randomized choice. We could not show the standard distribution of these morphologic parameters in the placental basal plate because the number of placentas studied was small. Identical protocols for the ART procedures were used in the 3 institutions; however, we cannot fully deny possible differences in subtle embryonic manipulations among laboratories.

In conclusion, artificial endocrinologic circumstances in frozen-thawed embryo transfer during the hormonal cycle may cause long-lasting changes in the placental basal plate and be causatively associated with the amount of bleeding in deliveries.

## Supplementary data

Supplementary data to this article can be found online at <http://dx.doi.org/10.1016/j.humpath.2015.04.007>.

## Acknowledgments

The authors thank Miss Chika Masuda, Miss Fukue Kondo, and Miss Teruyo Hosoya for their assistance in the random sampling of placentas and following assessment.

## References

- [1] Bower C, Hansen M. Assisted reproductive technologies and birth outcomes: overview of recent systematic reviews. *Reprod Fertil Dev* 2005;17:329-33.
- [2] Helmerhorst FM, Perquin DA, Donker D, Keirse MJ. Perinatal outcome of singletons and twins after assisted conception: a systematic review of controlled studies. *BMJ* 2004;328:261.
- [3] Jackson RA, Gibson KA, Wu YW, Croughan MS. Perinatal outcomes in singletons following in vitro fertilization: a meta-analysis. *Obstet Gynecol* 2004;103:551-63.
- [4] Lambert RD. Safety issues in assisted reproductive technology: aetiology of health problems in singleton ART babies. *Hum Reprod* 2003;18:1987-91.
- [5] Romundstad LB, Romundstad PR, Sunde A, et al. Effects of technology or maternal factors on perinatal outcome after assisted fertilisation: a population-based cohort study. *Lancet* 2008;372:737-43.
- [6] De Geyter C, De Geyter M, Steimann S, Zhang H, Holzgreve W. Comparative birth weights of singletons born after assisted reproduction and natural conception in previously infertile women. *Hum Reprod* 2006;21:705-12.
- [7] Shih W, Rushford DD, Bourne H, et al. Factors affecting low birthweight after assisted reproduction technology: difference between transfer of fresh and cryopreserved embryos suggests an adverse effect of oocyte collection. *Hum Reprod* 2008;23:1644-53.
- [8] Wang JX, Norman RJ, Kristiansson P. The effect of various infertility treatments on the risk of preterm birth. *Hum Reprod* 2002;17:945-9.
- [9] Thomson F, Shanbhag S, Templeton A, Bhattacharya S. Obstetric outcome in women with subfertility. *BJOG* 2005;112:632-7.
- [10] Zhu JL, Obel C, Hammer Bech B, Olsen J, Basso O. Infertility, infertility treatment, and fetal growth restriction. *Obstet Gynecol* 2007;110:1326-34.
- [11] Maheshwari A, Pandey S, Shetty A, Hamilton M, Bhattacharya S. Obstetric and perinatal outcomes in singleton pregnancies resulting from the transfer of frozen thawed versus fresh embryos generated through in vitro fertilization treatment: a systematic review and meta-analysis. *Fertil Steril* 2012;98:368-77 [1-9].
- [12] Schieve LA, Cohen B, Nannini A, et al. A population-based study of maternal and perinatal outcomes associated with assisted reproductive technology in Massachusetts. *Matern Child Health J* 2007;11:517-25.
- [13] Hayashi M, Nakai A, Satoh S, Matsuda Y. Adverse obstetric and perinatal outcomes of singleton pregnancies may be related to maternal factors associated with infertility rather than the type of assisted reproductive technology procedure used. *Fertil Steril* 2012;98:922-8.
- [14] Oron E, Ivanova N. Cell fate regulation in early mammalian development. *Phys Biol* 2012;9:045002.
- [15] Englert Y, Imbert MC, Van Rosendael E, et al. Morphological anomalies in the placentae of IVF pregnancies: preliminary report of a multicentric study. *Hum Reprod* 1987;2:155-7.
- [16] Jauniaux E, Englert Y, Vanesse M, Hiden M, Wilkin P. Pathologic features of placentas from singleton pregnancies obtained by in vitro fertilization and embryo transfer. *Obstet Gynecol* 1990;76:61-4.
- [17] Gavriil P, Jauniaux E, Leroy F. Pathologic examination of placentas from singleton and twin pregnancies obtained after in vitro fertilization and embryo transfer. *Pediatr Pathol* 1993;13:453-62.
- [18] Burton G, Saunders DM. Vasa praevia: another cause for concern in in vitro fertilization pregnancies. *Aust N Z J Obstet Gynaecol* 1988;28:180-1.
- [19] Williams H, Jeffery H. The incidence of histological chorioamnionitis in IVF/GIFT preterm births. *Aust N Z J Obstet Gynaecol* 1994;34:480-3.
- [20] Daniel Y, Schreiber L, Geva E, et al. Do placentae of term singleton pregnancies obtained by assisted reproductive technologies differ from those of spontaneously conceived pregnancies? *Hum Reprod* 1999;14:1107-10.
- [21] Cunningham FG, Leveno KJ, Bloom SL, Hauth JC, Rouse DJ, Spong CY, editors. *Parturition. Williams Obstetrics*. 23rd ed. New York: McGraw-Hill; 2010. p. 136-72.
- [22] Mayhew TM. Taking tissue samples from the placenta: an illustration of principles and strategies. *Placenta* 2008;29:1-14.
- [23] Altshuler G, Hyde SR. Clinicopathologic implications of placental pathology. *Clin Obstet Gynecol* 1996;39:549-70.
- [24] Furuta N, Yaguchi C, Itoh H, et al. Immunohistochemical detection of meconium in the fetal membrane, placenta and umbilical cord. *Placenta* 2012;33:24-30.
- [25] Benirschke K, Kaufmann P. *The pathology of the human placenta, nonvillous part and trophoblast invasion*. New York: Springer; 2000.
- [26] Wolska W. *Über die von Ruge beschriebene Vaskularisation der Serotina*. Bern: Thesis; 1888.
- [27] Rohr K. *Beziehungen der mütterlichen Gefässe zu den intervillösen Räumen der reifen Plazenta speziell zur Thrombose derselben ("weisser Infarkt")*. *Virchows Arch* 1889;115:505-34.
- [28] Sutcliffe RG, Davies M, Hunter JB, Waters JJ, Parry JE. The protein composition of the fibrinoid material at the human uteroplacental interface. *Placenta* 1982;3:297-308.
- [29] Nitabuch R. *Beiträge zur Kenntnis der menschlichen Plazenta*. Inaugural Dissertation. Bern: Stampfli; 1887.
- [30] Wynn RM. Fetomaternal cellular relations in the human basal plate: an ultrastructural study of the placenta. *Am J Obstet Gynecol* 1967;97:832-50.



REVIEW

# Nutritional conditions in early life and risk of non-communicable diseases (NCDs) from the perspective of preemptive medicine in perinatal care

Hiroaki Itoh, Naohiro Kanayama

Department of Obstetrics and Gynecology, Hamamatsu University School of Medicine, Hamamatsu, Japan

Reprint request to:

Hiroaki Itoh, M.D., Ph.D.,  
Department of Obstetrics and  
Gynecology, Hamamatsu  
University School of Medicine,  
1-20-1, Handayama, Higashi-ku,  
Hamamatsu, 341-3192, Japan.  
E-mail: hitou-endo@umin.ac.jp

Key words:

developmental origins of health  
and diseases (DOHaD), fetal  
origins of adult disease, fetus,  
pregnancy, thrifty phenotype

Received: December 11, 2014

Revised: February 3, 2015

Accepted: February 9, 2015

DOI:10.14390/jsshp.3.1

Non-communicable diseases (NCDs) are chronic diseases that are non-infectious and non-transmissible. The World Health Organization (WHO) classifies cardiovascular disorders (myocardial infarction or stroke), diabetes, chronic respiratory diseases, and malignancy as the four major disease types of NCDs. Evidence supporting the influence of various environmental factors in the early developmental period on the risk of developing NCDs in adults has increased recently, leading to the proposal of the developmental origins of health and disease (DOHaD) theory. We reviewed the background of the paradoxical circumstances in which the morbidity of NCDs has rapidly increased in both developing and developed countries in view of distinct prenatal nutritional environments in the context of the DOHaD theory. We also discuss candidates for early interventions and biological samples for identifying biological markers in individuals at high risk of NCDs from the perspective of preemptive medicine in perinatal care.

## Introduction

Non-communicable diseases (NCDs) are chronic diseases that are not passed from person to person and generally develop slowly over the course of life. The World Health Organization (WHO) proposed four main types of NCDs, i.e., cardiovascular diseases, diabetes, chronic respiratory diseases, and malignancy,<sup>1,2)</sup> in which obesity and metabolic syndrome are significantly involved. The WHO estimated that 63% of global deaths, approximately 36 million, were attributed to NCDs, and indicated that NCDs are expected to exceed communicable, maternal, perinatal, and nutritional diseases as the most common causes of death worldwide by 2030.<sup>1,2)</sup> The annual number of deaths due to NCDs continues to rise in both developing and developed countries.<sup>1-3)</sup> The recently developed theory of developmental origins of health and disease (DOHaD)<sup>4,5)</sup> proposed that nutritional conditions during the fetal, neonatal, and infantile periods are related to the NCD pandemic.<sup>6,7)</sup> In view of the DOHaD

theory, perinatal and neonatal medicine may help in the development of preemptive medicine against the rapid spread of adult NCDs.<sup>8,9)</sup> We herein discuss this possibility, as well as animal studies that support a nutritional imbalance *in utero* and in early postnatal life as a contributor to the recent NCD pandemic, with a particular focus on obesity and metabolic syndrome.

## Developmental Origins of Health and Disease (DOHaD) Theory

Epidemiological and animal studies revealed a possible association between environmental aggression in the early developmental period and the emergence of chronic diseases in later life. This concept suggests new links of causality and infers the early establishment of metabolic adjustments that determine morbidity throughout life, especially those causatively associated with NCDs,<sup>6,7)</sup> leading to a new branch of scientific knowledge known as the 'DOHaD' theory.<sup>4,10,11)</sup>

## Undernourishment in utero and risk of NCDs in later life

Epidemiological evidence connecting undernourishment *in utero* and the development of adult metabolic syndrome was initially obtained from victims of the Dutch Hunger Winter in 1944–5 during World War II. The adult and/or senile offspring of women exposed to the famine in gestation were predisposed to NCDs including coronary heart disease, obesity, impaired glucose tolerance, hypertension, an atherogenic lipid profile, disturbed blood coagulation, increased stress responsiveness, microalbuminuria, schizophrenia, and antisocial personality.<sup>12–14</sup> Fetal exposure to the Chinese Famine in 1959–61 was associated with a predisposition to hyperglycemia, type 2 diabetes, and metabolic syndrome in adulthood.<sup>15,16</sup> The association between fetal exposure to the Chinese Famine and an increased risk of adult metabolic syndrome was stronger among subjects with a Western style diet and/or those who were overweight in adulthood.<sup>17</sup>

Cohort studies identified a relationship between low birth weight and elevated adiposity in children<sup>18,19</sup> as well as adults;<sup>20–22</sup> however, small babies were not always simply the result of undernourishment *in utero*.

### ‘Thrifty phenotype’ hypothesis

Among the many mechanistic frameworks that have been proposed to explain the biological basis underlying possible associations between undernourishment *in utero* and obesity-related metabolic disorders in later life,<sup>23</sup> the ‘*thrifty phenotype*’ hypothesis by Hales and Barker<sup>24</sup> is the most compelling.<sup>25,26</sup> They proposed the concept of an adaptive response to fetal undernourishment that optimizes body growth *in utero* and leads to a permanently altered postnatal metabolic phenotype to match the predicted postnatal conditions of long-lasting poor nutrient supply and enhancing survivability throughout life under the circumstances of starvation<sup>24</sup> (Figure 1). Embryonic and/or fetal ‘*predictive adaptive responses*’<sup>27</sup> to suboptimal intrauterine undernourishment may promote permanently enhanced energy economy. This has been referred to as the ‘*thrifty phenotype*’. Regarding the ‘*matching*’ aspect of the ‘*thrifty phenotype*’ hypothesis, a previous study reported that small babies in Gambia, including those born during a nutritionally-debilitating hunger season, maintained excellent metabolic as well as cardiovascular conditions into adulthood with the complete absence of metabolic syndrome, provided that they retained their frugal lifestyle in rural areas.<sup>28</sup>

The ‘*thrifty phenotype*’ was proposed to only become detrimental when nutrition was more abundant in the postnatal environment than had been expected from

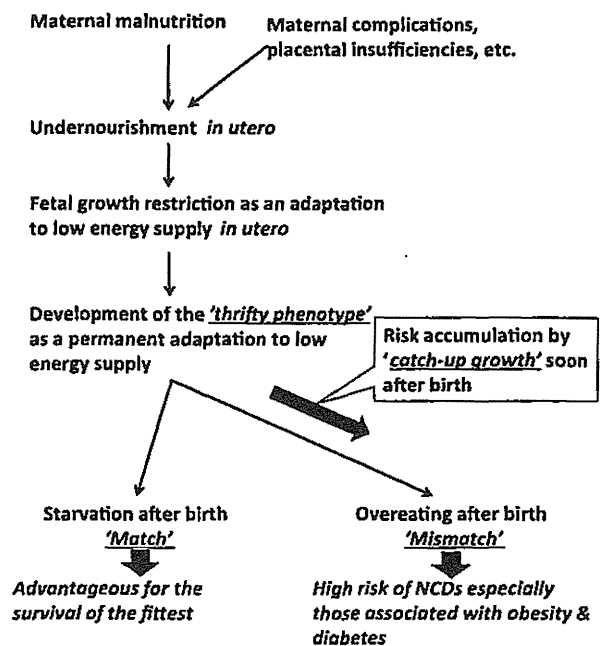


Figure 1. Relationship between undernourishment *in utero*, the ‘*thrifty phenotype*’, ‘*catch-up growth*’, and the risk of NCDs.

the prenatal environment of undernourishment because this phenotype for enhanced energy economy may lead to a ‘*mismatch*’ to the excess energy supply associated with the modern lifestyle of overeating, thereby predisposing adults to NCDs, especially those associated with obesity and/or type 2 diabetes<sup>24–26,29–32</sup> (Figure 1). Developing countries have been undergoing rapid economic improvements over the past few decades, and a generation that experienced a low nutritional environment during fetal life due to poverty and/or political turmoil has now shifted to a life of excess (Figure 2). Therefore, they are expected to have acquired the ‘*thrifty phenotype*’ *in utero* and now encounter a ‘*mismatch*’ of excess energy supply due to calorie-rich diets, thereby increasing the risk of NCDs associated with obesity and/or type 2 diabetes (Figure 1, 2).

In Japan, obesity has increased among adult males as well as mature and senile women, whereas undernourishment is common among women of childbearing age due to their strong desire to be thin,<sup>33</sup> concomitant with an increase in low birth weight neonates.<sup>32,34,35</sup> The mean total caloric intake of the Japanese population has continuously decreased since 1970,<sup>32,34</sup> indicating that the incidence of obesity has increased in spite of the intake of fewer calories. This paradoxical and rapid shift towards an obesity-prone phenotype in a relatively short period (i.e., less than half a century) in middle-aged and



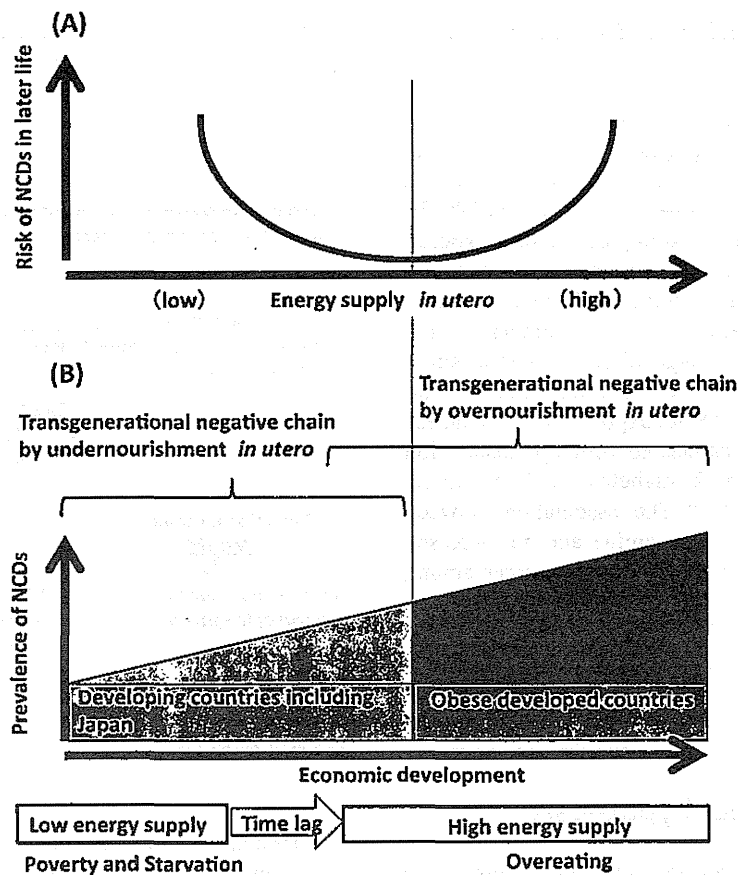


Figure 2. Energy supply *in utero* and the risk of NCDs in later life (A). The prevalence of NCDs in both developing and developed countries may be associated with differences in energy supply *in utero* (B).

elderly Japanese populations argues against the simple and major contribution of a Western lifestyle with a calorie-rich diet in favor of a presumed increase in the number of individuals with the 'thrifty phenotype' due to undernourishment *in utero*. Kubota et al.<sup>36)</sup> reported that the mean energy intake in Japanese pregnant women was less than 1,600 kilocalories/day throughout pregnancy, which corresponds to 30% (second trimester) and 37% (third trimester) fewer calories than what is recommended by the Ministry of Health, Labour and Welfare Japan (Figure 3). This suggests that considerable numbers of relatively undernourished Japanese fetuses exist due to a shortage in maternal energy intake. This distinct nutritional imbalance in Japanese pregnant women may have led to the 'thrifty phenotype' in a large number of Japanese people, contributing, at least partly, to the development of obesity and or type 2 diabetes with less caloric intake.<sup>35)</sup> Therefore, the nutritional conditions of Japanese fetuses are distinct from those in other developed countries, in which fetuses are typically supplied with excess energy from their mothers.

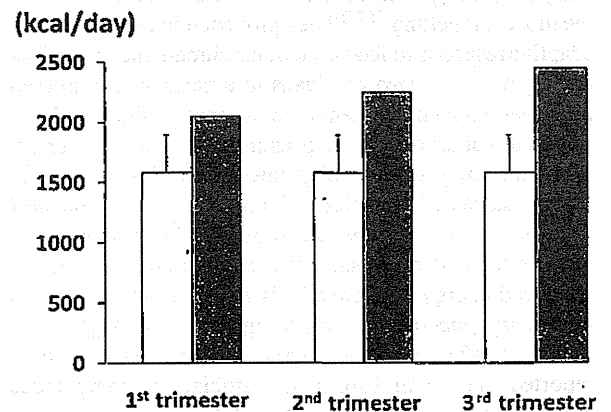


Figure 3. Mean energy intake of Japanese pregnant women in Hamamatsu city (white bars) and recommended energy intake by the Health, Labour and Welfare Ministry of Japan (gray bars).<sup>36)</sup> Error bars indicate standard deviations.

### 'Hypothalamic-adipose (HA) axis' hypothesis concerning 'thrifty phenotype'

The mechanisms underlying the 'thrifty phenotype' have not yet been elucidated in detail; however, large numbers of animal models have provided evidence to support its involvement in calorie-rich countries.<sup>37,38)</sup> Hales and Barker proposed that the permanently reduced secretion of insulin from pancreatic  $\beta$ -cells is critically involved in the development of an adult 'thrifty phenotype' concomitant with insulin resistance.<sup>24)</sup> Newsome et al.<sup>39)</sup> conclusively proposed a relationship between low birth weight and disorders in glucose and insulin metabolism in adulthood by a systematic review of the literature. However, the early-programmed reduced secretion of insulin does not coincide with the initial induction of obesity in later life because adipocytes require an appropriate amount of insulin to store lipids. Therefore, the fetal insulin hypothesis cannot fully explain the primary risk of obesity proposed by the 'thrifty phenotype' hypothesis.

Since the 'mismatch' of the 'thrifty phenotype' with an abundant energy supply may result in excess energy storage in the body, reasonably in adipose tissue, it is plausible that obesity is the most acceptable outcome of exposing 'thrifty phenotype' offspring to a calorie-rich diet. Moreover, obesity is a major risk factor for NCDs.<sup>40)</sup> Therefore, in this review, we focused on the developmental origins of obesity in relation to the 'thrifty phenotype', particularly in the context of the central regulation of energy metabolism, and introduced our 'hypothalamic-adipose (HA) axis' hypothesis as a candidate mechanism for explaining the acquisition of the 'thrifty phenotype'.

Obesity is closely associated with the regulation of food intake and energy expenditure, which are centrally regulated by the hypothalamus, the control center for energy metabolism. The adipocyte-derived hormone, leptin, is known to affect the hypothalamus, leading to a decrease in food intake and increase in energy expenditure.<sup>41,42)</sup> Disruptions in the production and circulating levels of leptin have been shown to play an important role in the development of metabolic syndrome in adulthood.<sup>41)</sup> Evidence obtained in animal studies supported undernourishment *in utero* causing low hypothalamic sensitivity to circulating leptin, thereby linking undernourishment *in utero* to the risk of obesity in later life.<sup>43)</sup> Moreover, maternal caloric restriction did not exacerbate obesity in leptin-deficient *ob/ob* mice, suggesting that leptin is a key factor in the developmental origins of obesity.<sup>44)</sup> We previously revealed that undernourishment *in utero* resulted in blunted responses in food intake by and lower body weights in adult mice treated with leptin, concomitant with low signal transduction responses in the hypothalamus, relative

to normally nourished controls.<sup>45)</sup> We also showed that chemical damage to the arcuate nucleus (ARC) of the hypothalamus canceled out the accelerated development of obesity in adult mouse offspring that were undernourished *in utero*.<sup>45)</sup> Since the ARC, which centrally regulates energy expenditure,<sup>46)</sup> has been proposed to be the main target of leptin, permanent changes in hypothalamic responsiveness to circulating leptin appear to be the main regulatory system in the developmental risk of adult obesity, at least in our mouse animal model of undernourishment *in utero*.

Serum leptin levels markedly increase in normal mouse neonates during the lactation period, and this is referred to as the 'leptin surge'<sup>47)</sup> (Figure 4A). However, previous studies reported that leptin did not affect feeding or thermogenesis in neonatal mice<sup>48)</sup> or rats.<sup>49)</sup> Bouret et al.<sup>50)</sup> reported that the neurotrophic action of leptin in the mouse hypothalamus only operated during the neonatal period. We<sup>44,45)</sup> and others<sup>51,52)</sup> proposed that undernourishment *in utero* changed the timing and/or plasma levels of leptin in the 'leptin surge' during the period of lactation and modified the development of neuronal circuitries in the hypothalamus, resulting in permanently low hypothalamic responses to circulating leptin and thereby increasing the risk of obesity (Figure 4B). However, changes in the 'leptin surge' during the neonatal period and its permanent effects on adulthood

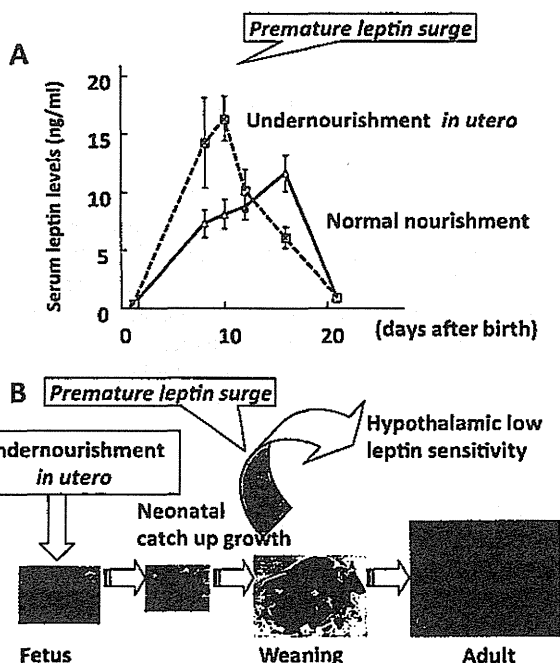


Figure 4. The 'Hypothalamic-adipose (HA) axis' hypothesis as a possible mechanism underlying acquisition of the 'thrifty phenotype'.<sup>32,45)</sup>

remain controversial. We previously demonstrated that a 30% restriction in maternal caloric intake (70% of *ad libitum* intake) in the latter half of pregnancy caused earlier and greater deviations in the 'leptin surge' in neonates, which we described as a 'premature leptin surge'<sup>45)</sup> (Figure 4A). To examine the relationship between the 'premature leptin surge' and the risk of adult obesity, we administered leptin to normally-nourished male mice aged 5 to 10 days and found that these pups subsequently developed a similar obesity-prone phenotype and low hypothalamic sensitivity to leptin as pups undernourished *in utero*, concomitant with similar changes in the development of neuronal circuitries in the hypothalamus.<sup>45)</sup> These findings suggested a distinct role for the 'premature leptin surge' as a programming signal from adipose tissue to the hypothalamus. De Moura et al.<sup>52)</sup> also reported that the treatment of neonatal rats with leptin, either from 0 to 10 days of age or in the last 10 days of the lactation period, led to obesity and high leptin concentrations in later life.

On the other hand, Delahaye et al.<sup>51)</sup> reported that a 50% restriction in caloric intake by rats from pregnancy to the lactation period markedly decreased the 'leptin surge'. Vickers et al.<sup>53)</sup> administered leptin to rat neonates from 3 to 10 days and found no phenotypic changes in normally nourished pups, but protection against obesity in pups undernourished *in utero*. To the best of our knowledge, there is currently no clear explanation for this discrepancy and we speculate the presence of multifactorial 'critical windows' in exposure of the hypothalamus to the 'leptin surge' during the lactation period with respect to timing, duration, dosage of the leptin treatment in each experimental protocol, gender differences, and species differences even between rats and mice. Nevertheless, changes in plasma leptin concentrations during the lactation period induced by fetal undernourishment, although still contentious, appear to be a key modulator of permanent hypothalamic energy regulation, leading to the development of the obesity-prone adult phenotype. Based on our findings, we proposed the important contribution of the 'HA axis' hypothesis to the developmental origins of obesity (Figure 4B).

### 'Hypothalamic-pituitary-adrenal (HPA) axis' hypothesis and NCDs

The hypothalamus is not only the center of energy metabolism, but also a central regulator of stress responses that down-regulate the secretion of glucocorticoids from the adrenal glands, i.e., the hypothalamic-pituitary-adrenal (HPA) axis. A shift to an elevated stress response has been closely linked with the risk of NCDs.<sup>54-57)</sup> The findings of previous clinical and molecular studies

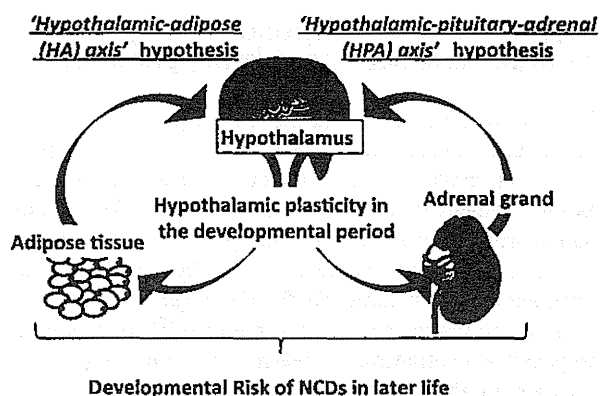


Figure 5. Hypothalamic plasticity in early life and developmental risk of NCDs in later life.<sup>32)</sup>

demonstrated that elevated levels of adrenal hormones caused the accumulation of fat in visceral adipose tissues as well as associated metabolic abnormalities.<sup>58,59)</sup> Human and animal studies indicated that prenatal stress caused the permanent hyper-reactivity of the HPA axis to be causatively associated with an elevated risk of NCDs; namely, the 'HPA axis' hypothesis<sup>60-68)</sup> (Figure 5).

Morphological and functional hypothalamic plasticity during the early developmental period has been suggested to play a key role in the 'HPA axis' and 'HA axis' hypotheses (Figure 5); therefore, the hypothalamus appears to be a promising target organ in the search for new early interventions that will reduce the prevalence of NCDs.

### Accumulation of NCD risk by 'catch-up growth'

A systematic review revealed that small babies were more predisposed to adult obesity if they showed rapid 'catch-up growth' soon after birth<sup>69)</sup> (Figure 1). Regarding the critical period of 'catch-up growth', previous studies suggested the possible importance of the first few weeks of postnatal life<sup>70,71)</sup> or the period until two years of age,<sup>69)</sup> whereas others showed that low birth weight children who grew excessively in later childhood were also at a higher risk of adult obesity.<sup>21,72)</sup> Botton et al.<sup>73)</sup> showed that neonates with a faster weight gain velocity during the first three months showed a greater weight gain velocity after three years of age, leading to a larger fat mass in adolescence (Figure 6). These findings suggested that the interaction between prenatal low energy supply and subsequent rapid 'catch up growth' soon after birth, presumably being equal to a rapid encounter with a postnatal high-energy supply, appeared to increase the risk of obesity and its associated metabolic disorders<sup>31,38,74-76)</sup> (Figure 1).

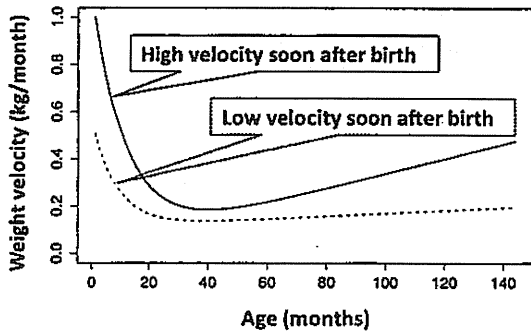


Figure 6. Predicted transition of weight growth velocity (modified from the figure by Botton et al.)<sup>73)</sup>

**'Catch-up-related adipose tissue remodeling' hypothesis concerning accumulation of NCD risk by 'catch-up growth'**

To the best of our knowledge, a consensus has not yet been reached regarding how 'catch-up growth' soon

after birth increases the risk of adult obesity caused by undernourishment *in utero*, or how it permanently modulates the metabolic characteristics of the 'thrifty phenotype' acquired by undernourishment *in utero*. We recently focused on the possible involvement of adipose tissue remodeling in the aggravation of obesity-related metabolic disorders by 'catch-up growth' during the lactation period.

The fat body of drosophila evolved into three different organs, i.e., adipose tissue, liver, and blood cells of mammals, over a period of 60 million years, during which the reciprocal regulation of their functions developed.<sup>77)</sup> Recent studies identified various changes in the intercellular spaces between ballooning adipocytes due to increased lipid storage, particularly those associated with the chronic infiltration of immune competent cells, especially inflammatory macrophages, leading to the concomitant impairment of glucose and/or lipid metabolism.<sup>78-80)</sup> We recently developed a mouse animal model of undernourishment *in utero* by maternal caloric restriction, in which the rate of 'catch-up growth' during the lactation period positively correlated with

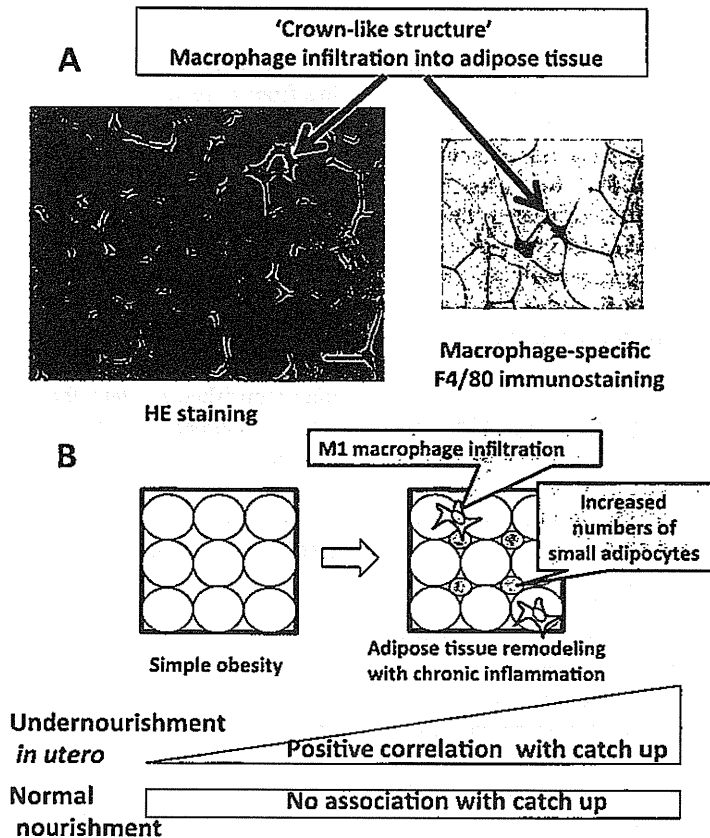


Figure 7. 'Catch-up-related adipose tissue remodeling' hypothesis for increased risk of obesity and associated metabolic disorders by 'catch-up growth'.<sup>81,84)</sup>